*Manuscript

Reverse Osmosis Desalination of Brackish Agricultural Drainage Water in the San Joaquin Valley

Brian C. McCool[1], Anditya Rahardianto[1], Jose Faria[2], Kurt Kovac[2], David Lara[2], and Yoram Cohen[1*]

[1] Water Technology Research Center, University of California, Los Angeles, CA, USA

[2] California Department of Water Resources, Fresno, CA, USA

Desalination

[*] Corresponding Author, Tel.: +1 (310) 825-8766; E-mail: yoram@ucla.edu

Abstract

The technical feasibility of reverse osmosis (RO) desalination of agricultural drainage (AD) water in California's San Joaquin Valley (SJV) was evaluated based on systematic analysis of water quality monitoring data and field water desalting tests in a laboratory plate-and-frame RO (PFRO) system. Thermodynamic solubility analysis and diagnostic PFRO desalting tests served to determine the feasible range of water recovery limits and to assess the mineral scaling potential. Analysis of the recovery limits imposed by scaling due to sparingly soluble salts (e.g. calcite, gypsum, silica) suggested feasible recoveries in the range of 46%–69%. Diagnostic PFRO desalting tests with five representative field water sources from the SJV (having gypsum and calcite saturation indices in the range of 0.12–1.03 and 2.9–9.5, respectively) confirmed the above recovery range. Mineral scale coverage was consistent with the observed flux decline. Deployment of RO technology for treatment of brackish SJV AD water would require site-specific process optimization given the geographic and temporal water quality variability. Therefore, RO operation with variable feed water quality (with respect to salinity and scaling propensity) and at sufficiently high recovery would require effective plant control, enabled by real-time mineral scale detection and adaptable process operation to mitigate mineral scaling.

Keywords: desalination, reverse osmosis, recovery limits, brackish water, mineral scaling

1. Introduction

The San Joaquin Valley (SJV) in central California (see Fig. 1) is one of the United States' most productive agricultural regions [1, 2]. Decades of irrigation and evapotranspiration combined with a shallow water table and naturally saline soil have led to the rise in groundwater salinity in the SJV. As the brackish water table intrudes into the root-zone increasing the soil salinity, many crops are adversely affected. When the salinity tolerances of the crops are exceeded the land is often retired, progressively diminishing the productivity of the SJV [3-6]. The rising groundwater salinity level in the SJV, now in the range of about 3,000–30,000 mg/L total dissolved solids (TDS), is a problem of major concern [5-7]. In order to reduce further buildup of salt in the soil, beginning in the late 1940s, surface and subsurface drains were installed throughout the valley to collect the brackish agricultural drainage (AD) water and then convey it to evaporation ponds or other discharge sites; by 1965 more than 1000 miles of drains had been built [4]. Construction of a master drain discharging to the Sacramento-San Joaquin River Delta was stopped in 1983 after the drainage from a preliminary portion of the drain that had been discharging into the Kesterson Reservoir was found to contain high levels of Selenium [4, 6, 8]. Although it is noted that where natural drainage does not exist the use of evaporation ponds or other discharge sites for high salinity drainage water has become infeasible due to concern regarding bioaccumulation of selenium [4, 6, 8].

In recent years there has been a renewed interest in the use of reverse osmosis (RO) and nanofiltration (NF) membrane desalination of SJV brackish groundwater as a potentially viable approach for reclamation of AD water for agricultural reuse and possibly potable water consumption [7], while also reducing the challenge of concentrate (brine) management. As the percentage recovery of permeate product of the RO process is increased the volume of brine discharge is decreased. However, the achievable RO recovery may be limited because SJV

brackish water is often near or above saturation with respect to various sparingly water soluble mineral salts such as gypsum ($CaSO_4 \cdot 2H_2O$), calcium carbonate ($CaCO_3$), silica (SiO_2), and barite ($BaSO_4$). Upon RO desalting, the concentration of such salts on the feed-side and near the RO membrane surface can increase to levels exceeding their solubility limits which can then lead to surface crystallization of these mineral salts and/or the deposition of their bulk-formed crystals onto the membrane surface. The resulting mineral surface scale leads to water permeate flux decline and potential damage to the membrane [9-14]. Consequently, the feasible recovery limit and process efficiency are reduced and water production costs increase. Given that the composition of SJV brackish water varies with location and time (e.g., with respect to salinity and the composition of sparingly soluble mineral salts) the mineral scaling propensity of such water is also location and time-dependent.

In order to assess the technical feasibility of RO desalination of SJV brackish water, there is a need to evaluate the product water recovery limits that are imposed by mineral salt scaling. Accordingly, in the present study, SJV AD water from a number of representative geographical locations was first characterized using available monitoring data for the 1999–2004 period with respect to composition, mineral salt saturation levels, and temporal variability. Based on RO process considerations, the upper limits on water recoveries were first estimated based on thermodynamic solubility analysis. Subsequently, laboratory bench-scale plate-and-frame RO (PFRO) mineral scaling tests were performed using water samples from five different representative locations to confirm the scaling propensity of SJV AD water and establish the expected range for the upper level of RO recoveries.

2. Analysis of RO Desalination Recovery Limits

Product water recovery limits governed by mineral salt scaling can be estimated given knowledge of the water feed chemistry in order to establish the threshold for mineral scaling. In brackish water desalination the maximum allowable pressure for the membrane modules (typically 4140 kPa or 600 psi) may also dictate a practical limit on recovery that may be above or below the limit dictated by mineral scaling. Increased product water recovery, Y, of an RO desalination process (defined as $Y = Q_P/Q_F$ where Q_P and Q_F are the permeate and feed flow rates, respectively) increases the average mixed-cup concentration of the retentate (or brine) stream, C_R, by a factor CF relative to the feed concentration, C_F (i.e., $CF = C_R/C_F$). This concentration factor is related to the recovery and salt rejection, R_S ($R_S = 1 - C_P/C_F$, where C_P is the permeate concentration), by

$$CF = \frac{1 - Y(1 - R_S)}{1 - Y} \tag{1}$$

As recovery increases, the retentate concentration in the membrane channel can increase to levels such that sparingly soluble mineral salts can exceed their saturation concentrations (Fig. 2), and precipitate in the bulk or crystallize onto the membrane surface [15, 16], thereby resulting in membrane scaling which reduces permeate flux and can also shorten the membrane life [17-19]. Mineral salt scalants that are of particular concern in brackish water desalination include gypsum ($CaSO_4 \cdot 2H_2O$), calcium carbonate ($CaCO_3$), and barite ($BaSO_4$) in addition to scaling by colloidal silica [17-20]. The recovery limits for a given feed water source can be estimated using Eq. (1) by establishing the CF at which the retentate concentrations reach the mineral salt scaling thresholds. The above approach provides an upper limit estimate of the feasible recovery since it does not consider the impact of concentration polarization [21].

Concentration polarization results in higher salt concentrations at the membrane surface relative to the bulk solution; thus, a lower recovery limit would result relative to the estimate from Eq. (1) which is based on the on a mixed-cup average retentate concentration. Membrane manufacturers typically specify that the concentration polarization modulus, *CP* (=C_M/C_B, where C_M and C_B are the salt concentrations at the membrane surface and in the bulk of the membrane channel, respectively) in a given spiral-wound element be no greater than about 1.20 [22]. In order to estimate recovery limits while considering the additional impact of concentration polarization, one can define a concentration polarization modulus allowance [22, 23] at the exit region of the tail element as $C_M = \alpha C_R$, where α is a concentration polarization allowance factor.

In order to estimate RO permeate recovery, based on information from an overall salt mass balance or desalting tests in small plate-and-frame RO systems with negligible recovery, a simple approach is proposed to provide a reasonable estimate of the equivalent recovery expected in RO plants. Accordingly, when a *CF* threshold is established based, for example, on the maximum allowable mixed-cup retentate concentration (e.g., due to solubility or pressure constraints) one must correct the estimate from Eq. (1) to account for concentration polarization. Accordingly, *CF* can be adjusted by introducing a concentration polarization allowance factor ($\alpha = C_M / C_R$, where C_R is the mixed-cup retentate salt concentration) such that CF / α replaces *CF* in Eq. (1).

The mineral scaling threshold dictates the maximum allowable recovery and is expressed in terms of the saturation index, SI_i, for the limiting mineral salt *i*, defined as

$$SI_i = \frac{IAP_i}{K_{SP,i}} \tag{2}$$

where IAP_i is the ion activity product of the constituent ions and $K_{SP,i}$ is the solubility product. The RO feed is often dosed with antiscalant (AS) additives to enable RO operation at or above

saturation (i.e. $SI_i \geq 1$). Therefore, the scaling threshold is typically taken to be the *SI* above which membrane scaling is likely to occur even in the presence antiscalant. For example, recommended scaling thresholds, with the appropriate antiscalant use, for gypsum, barite, and silica are SI_G = 2.3–4.0, SI_B = 60–80, and SI_S = 1.0–3.0 respectively [24]. The pH dependence of the saturation indices for calcite, gypsum, barite, and magnesium hydroxide are shown in (Fig. 3) for a representative water sample from a specific site (OAS, Table 3) in the SJV (Fig. 1). The saturation indices for gypsum and barite are pH insensitive while calcite and magnesium hydroxide saturation indices are highly dependent on pH. Therefore, the SI_C can be adjusted to desired levels by pH adjustment of the feed. Magnesium hydroxide, however, is well below saturation ($SI < 0.001$) over the expected range of operating pH for RO processes (pH 6–8) and therefore it is not likely to impact the recovery limits. The saturation indices for barite are upper limits, given that barium concentrations for the above water source were reported at or below the detection limit (i.e., 0.25 mg/L). It is noted that although thermodynamic solubility analysis suggests that SI_C can be reduced by acid dosing, recent work [7] has shown that operating at reduced pH in waters of high gypsum scaling propensity but low in carbonate may be counterproductive; for such a water source, the rate of gypsum precipitation may increase due to the decreased bicarbonate concentration, thereby leading to a reduction in bicarbonate's tendency to retard gypsum precipitation.

Estimates of recovery from experimental studies with a traditional plate-and-frame RO (PFRO) system are also feasible to obtain, despite the typically low recovery in such units (≤ 1–2%), since a relatively high level of concentration polarization may be achieved even in such small systems. The equivalent recovery in a full-scale RO system can be estimated from PFRO data as the recovery at which a full-scale RO system would experience a concentration at the membrane surface at the exit region equivalent to the average membrane surface concentration in

the PFRO system. The average surface concentration for the PFRO cell is calculated based on the average concentration polarization modulus, $\overline{CP}$, (defined as $\overline{CP} = \bar{C}_M / C_B$ where $\bar{C}_M$ is the average membrane concentration) using the numerical procedure developed specifically for the present RO cell geometry [21]. The equivalent recoveries are then calculated using Eq. (1), replacing $\overline{CP}$ by *CF*, with α = 1.0 or 1.2 (i.e., without and with concentration polarization allowance to yield reasonable upper and lower limit recovery estimates, respectively). In order to determine if mineral scaling should be expected at the operating conditions in the PFRO, the saturation indices at the membrane surface, $\overline{SI}_i$, for the mineral salts of concern may be calculated accounting for $\overline{CP}$ as below:

$$\overline{SI}_{M,i} = \frac{IAP_{M,i}}{K_{SP,i}} = \frac{\overline{CP}^n}{K_{SP,i}} \prod_j C_{B,j} \gamma_j \tag{6}$$

where $IAP_{M,i}$ is the ion activity product at the membrane surface for mineral salt *i*, $C_{B,j}$ is the bulk concentration of mineral salt's constituent ion *j*, γ_j is the ion activity coefficient at the membrane surface, and *n* is the number of ions contained in mineral salt *i*. The above approach assumes that the level of concentration polarization is the same for all ions, a simplification that is reasonable for estimation purposes. Finally, it is noted that in the present work, the saturation indices and osmotic pressures were calculated using a multi-electrolyte thermodynamic simulation software [25].

3. Materials and Methods

3.1 Materials & Reagents

Stock solutions of hydrochloric acid (1.0 M) and sodium hydroxide (0.1 M) were prepared from concentrated hydrochloric acid (22° Bé, technical, Fisher Scientific) and sodium

hydroxide pellets (A.C.S. reagent, Sigma Aldrich), respectively, in DI water for pH adjustment of field water samples. The antiscalant PC-504 (Nalco Company, Naperville, IL) was used in some of the scaling tests at a low dose of 0.2 ppm to demonstrate the impact on scale inhibition. Agricultural drainage water field samples from five selected San Joaquin Valley locations were provided by the California Department of Water Resources (DWR) [26] and were refrigerated and maintained at 5ºC prior to use. Analyses of metals, anions, alkalinity, total organic carbon (TOC), and silica were performed using methods published in Standard Methods for the Examination of Water and Wastewater [27] or using USEPA analytical methods for drinking water [28]. All water quality data were reconciled to ensure charge balance and pH consistency [25].

All RO desalting tests were carried out using the LFC-1 (Hydranautics, Oceanside, CA) brackish water RO membrane because of its low biofouling potential, high permeability, and high salt rejection [17]. This membrane has a reported permeability of $9.8 \pm 0.3 \times 10^{7}$ $m \cdot bar^{-1} s^{-1}$, a salt rejection of ~98% (based on electrical conductivity measurements for desalting of field water samples), and a root-mean-square (RMS) surface roughness of 67.4 nm [29, 30]. Membrane compaction/conditioning was accomplished using solutions of sodium sulfate (certified A.C.S anhydrous, Fisher Scientific, Pittsburgh, PA) in de-ionized water following previously established procedures [7, 19, 30].

3.2 PFRO System & Mineral Scaling Tests

The laboratory plate-and-frame RO (PFRO) membrane system consisted of two reverse osmosis cells arranged in parallel. Details of the system are described elsewhere [7, 19, 30]. Briefly, each of the RO cells had an effective membrane surface area of 19.8 cm^2 (2.6 cm x 7.6 cm) with a channel height of 2.6 mm. The feed was pressurized by a ¾ hp positive displacement

pump (Dayton Electric Mfg. Co., Niles, IL). A bypass valve allowed regulation of the feed flow rate to the reverse osmosis cells. Pressure in the cells was regulated by a backpressure valve in place following the recombination of the two parallel retentate streams. The feed reservoir was continuously stirred and temperature controlled (±0.5 °C) using a refrigerated recirculator (Fisher Scientific, Pittsburg, PA). All RO experiments were carried out in a total recycle mode with the permeate and retentate flow rates monitored using a digital flow meter and a rotameter, respectively. The retentate from the PFRO cells was filtered using a 0.2 µm Nylon filter cartridge prior to being diverted to the feed tank. This was done as a precautionary measure in order to remove any mineral scale crystals that may have formed in the bulk (on the feed-side of the membrane) or dislodged from the membrane surface. Feed pH was measured with a pH electrode (Cole Parmer Instrument Company, Vernon Hill, IL) and conductivities (of the permeate and feed) were measured using a conductivity meter (model WD-35607-30, Oakton Research, Vernon Hills, IL). Optical images of the dried membranes were obtained using a high-resolution digital camera (Nikon model D100, Nikon Corp., Japan) with a 28–105 mm lens and a 4+ macro lens attachment and high contrast imaging of the scaled surface was achieved using a low angle dark-field illuminator as described in previous work [30].

RO desalting tests with the field water sources (Table 7) were carried out at the natural field water pH and at acidic conditions (pH range ~5.3–6.5, $SI_C \leq 0.37$) both with and without a low dose of antiscalant (0.2 ppm). Prior to each RO test each field water sample was pre-filtered successively through a 5-µm gradient-density polypropylene filter cartridge and then a 0.2 µm pleated Nylon filter cartridge (Cole-Parmer Instrument Company, Vernon Hills, IL) to remove suspended particles. In order to reduce pH drift (during the experiments performed at a reduced pH) air was bubbled through the water feed reservoir during pH adjustment to reduce the time to reach equilibrium with respect to carbon dioxide. Membranes used in the PFRO cells were cut

from a commercial stock membrane roll. The membrane coupons were rinsed with ~500 mL of DI water and then soaked in DI water for at least two hours prior to placement in the RO cells. Prior to each desalting run, the membrane coupons were placed in the RO cells and conditioned with a sodium sulfate solution having approximately the same osmotic pressure as the field water solution. Membrane compaction was carried out at a retentate flow rate of about 4.5 L/min (average cross-flow velocity, $\bar{u}$, of 110 cm/s) for an hour and then for three hours at retentate and permeate flow rates necessary to produce the desired equivalent recovery in the subsequent RO desalting tests (see Eq. 1). After membrane conditioning, each RO test was initiated to attain an average concentration polarization level, $\overline{CP}$, in the range of 1.6–2.1 for each feed water sources. The series of RO desalting tests for each given water source were carried out at the same initial flux and cross flow velocity in order to ensure flux decline comparisons at the same initial level of concentration polarization and thus the same initial saturation index with respect to gypsum (which was not influenced by pH adjustment). The initial average saturation indices for calcite, gypsum, and silica, at the membrane surface ($\overline{SI}_{M,C}$, $\overline{SI}_{M,G}$, $\overline{SI}_{M,S}$, respectively) were estimated based on the average concentration at the membrane surface (Eq. (6)). The percent flux decline as a function of time, $FD_t = (1 - J_t/J_0)\cdot 100$ (where J_0 and J_t are the initial flux and the flux at time t, respectively) was determined for each RO desalting test in order to assess the impact of scaling and membrane compaction. The percent of the membrane covered by scale after the 24-hr test period, ϕ_{24}, was also determined based on image analysis of the scaled membranes. The experimental conditions are provided in Table 7.

3.3. Water Quality Data

Two data sets were utilized to assess brackish water quality at different locations in the SJV: (a) California Department of Water Resources (DWR) monitoring data from 1999–2004

from which four representative sites were identified [26, 31], and (b) field water sampling data collected during 2006–2007 from five sites (four were the same sites identified in (a)) specifically for the present study (Fig. 1). The DWR monitoring data were reviewed to evaluate temporal and geographic variability of water quality and the implications for RO recovery limits, specifically for the latest 12-month period for the representative sites identified from the DWR drainage monitoring data. These four sites were selected as being representative of the diversity of water compositions with respect to salinity (i.e. TDS), gypsum saturation index, and calcite saturation index. However, because the monitoring database [4] lacked information on the concentrations of bicarbonate, carbonate, hydroxides, and silica, and given the temporal variability of water quality, experimental RO desalting tests, for water sources from the field locations in the SJV, were carried out for field samples collected during the testing period (2006–2007).

4. Results and Discussion

4.1 Water Quality Variability

Brackish groundwater monitoring data for four representative monitoring sites in the SJV were analyzed with respect temporal and spatial variations in water quality and to assess the potential range of RO recovery limits. These sites designated by DWR as CNR 0801, LNW 6467, OAS 2548, and VGD 4406, hereafter referred to as CNR, LNW, OAS and VGD, respectively, are shown in Fig. 1. Thermodynamic solubility analysis was performed for the latest 12-month period of the 1999–2004 data and for the 2006–2007 field samples which included, in addition to the above sites, a water source sample from site ERR 8429 [4], referred to as ERR (Fig. 1).

AD water quality for the 1999-2004 period exhibited significant spatial variability among the monitoring sites (Table 1). Analysis of the latest 12-month period of data (for each site) revealed that average salinity from the selected sites ranged from 6,987 to 23,480 mg/L total dissolved solids (TDS) for the CNR and VGD sites, respectively, with corresponding average osmotic pressures ranging from 315–1000 kPa (45.7–145 psi). All water sources were oversaturated with respect to calcite with the average SI_C ranging from 2.3 to 5.3 (Table 1) and near saturation with respect to gypsum with the average SI_G in the range of 0.75–0.99 (OAS and LNW sites, respectively). The above spatial variations are significant in both osmotic pressure and saturation indices suggesting that RO operating conditions (which will impact the cost of water desalination) must be tailored for each specific location within the SJV.

Water quality also varies temporally as illustrated in Fig. 5 where the percent deviation from the 12-month average values is shown for the selected field. As an example, detailed water quality data for one of the sites OAS), for the latest 12-month period of available data (from the DWR monitoring database), is provided in Table 2. Water salinity exhibited maximum absolute deviations from the 12-month averages ranging from 12% to 52% for LNW and OAS, respectively, and the maximum osmotic pressure deviations were in the range of 10%–44%. Both calcite and gypsum saturation indices varied substantially over the 12 month periods for the selected sites. The maximum absolute deviation of SI_C relative to the average ranged from 54% to 92% for VGD and CNR, respectively, while the maximum absolute deviation of SI_G from the 12-month average was in the range of 3.3%–45% for CNR and OAS, respectively. The SI_C variations were primarily due to pH fluctuations, while SI_G variations were primarily due to fluctuations in calcium and sulfate ion concentrations. These large temporal variations in water quality (e.g., salinity and saturation indices) would prove challenging to traditional RO plants that are typically designed to process water of a relatively narrow range of salinity and mineral

scaling propensity. As water quality changes, the osmotic pressure and saturation indices vary and will affect the energy consumption (proportional to the feed osmotic pressure and desired recovery), required chemical doses, and scaling recovery limits. Analysis of the 2006–2007 sampling data revealed that the water quality of the more recent samples fell largely within the ranges established for the earlier DWR database (Table 3, Fig. 5). The detailed water quality analysis for each of the five locations in the SJV is listed in Table 4.

4.2 Recovery Limits for the 1999–2004 and 2006–2007 Monitoring Data

RO recovery limits based on the highest and lowest reported salinity for each field location (Fig. 1) over the latest 12-month period for the DWR 1999–2004 monitoring data set are summarized in Table 5. The recovery limits based on scaling thresholds for gypsum were computed for SI_G =1 (without AS use) and SI_G = 2.3 (with AS use) and for calcite at SI_C = 1.0 (assumed to be achievable via pH adjustment). Recovery limits were calculated at both the field water pH = 7.5 and at a reduced pH = 6.0 to illustrate the effect of pH adjustment. At the natural pH, calcite is the limiting scalant. However, a pH = 6.0 gypsum becomes the limiting scalant with desalting being either infeasible (e.g., LNW feed $SI_G \approx 1$) or limited to low recoveries (Table 5) with the highest recovery being 44%–53% (for α = 1.2 and 1, respectively, Section 2) for OAS. When the gypsum scaling threshold is set at the level allowable with antiscalant treatment (i.e., SI_G = 2.3), the recovery limits increase to the range of 43%–76% or 53%–80% with and without allowance for concentration polarization, respectively. It is noted that the osmotic pressures at the scaling recovery limits for each of the sites are well below 4140 kPa (600 psi), the typical pressure limit for brackish water RO modules. The above analysis indicates that variability in water quality (temporally and geographically) would require site-specific plant

design in addition to effective feed-back process control to handle variability in feed water quality.

In order to further assess the impact of changes in water quality on RO recovery limits, the five locations in the SJV (Fig. 1) were sampled over the 2006–2007 season with the water quality data provided in Table 4. Recovery limits were estimated based on gypsum scaling thresholds of SI_G = 1 (without AS use) and SI_G = 2.3 (with AS use), silica scaling threshold of SI_S = 1, and calcite scaling threshold of was SI_C = 1.0. Product water recoveries were calculated at both the natural source water pH, which ranged from 7.5 to 8.0 among the five selected sites, and at a reduced acidic pH of 6.0. Each of the brackish water sites were oversaturated with respect to calcite at the natural field water pH (Table 6) implying that feed acidification would be required to lower the saturation index with respect to calcite. However, even if calcite scaling is inhibited gypsum would remain the limiting scalant with estimated lower and upper recovery ranges of 44%–62% and 54%–68% with and without CP allowance (Section 2), respectively, except for the ERR site for which silica was the limiting scalant (Table 6) even with gypsum scale mitigation with antiscalants (allowing operation up to ~ SI_G=2.3). Estimated product water recovery limits due to gypsum scaling range from being infeasible for LNW (SI_G = 1.03; Table 3) to as high as 63% for ERR. However, even at the higher gypsum scaling threshold (SI_G = 2.3 with AS treatment) gypsum remains the limiting scalant for CNR, OAS, and LNW, while silica was the limiting scalant for both the ERR and VGD samples. The overall recovery limits when considering both gypsum and silica scaling are between 46% and 77% consistent with the estimated recovery limits determined based on the 1999–2004 DWR monitoring data. It should be noted that in all cases (Table 6), if the operating pressure is limited by the typical rating of the brackish water RO vessels (4140 kPa or 600 psi), the recovery limit would be higher than that which would be imposed by mineral scaling. Water quality data obtained over the 2006–2007

period of the current study confirmed that geographic variability of brackish water quality in the SJV is significant as was determined for the 1999–2004 data set with recovery limits (53–80%) imposed by gypsum and silica scaling.

4.4 Experimental RO Desalting Tests

In order to confirm the estimated range of water recovery feasible for the SJV (Section 2), RO desalting tests were performed with field water samples (Table 3) at the natural source water pH, and at a reduced pH with and without a low dosage of antiscalant over the range of operating conditions indicated in Table 7. These tests targeted equivalent recoveries in the range of about 38%–53% for which the average saturation index for gypsum at the membrane surface was in the range of 1.4–2.1. Desalting tests at the reduced pH along with AS dosing of the feed revealed about 7%–9% flux decline after 24 hours (FD_{24}) and no observed mineral scaling (Table 7) despite the level of supersaturation of the solution at the membrane surface (e.g., up to $\overline{SI}_{M,G}$ = 2.1 for ERR, CNR and OAS). Previous work with the LFC1 membrane has shown that typically up to about 5–7% flux decline could be the result of membrane compaction [30]. Therefore, it is likely that a major contribution to flux decline for the above desalting tests (and other tests for which no scaling was visually observed; Table 7) was from compaction with possibly low levels of colloidal or organic fouling (7–9%). In contrast, significant flux decline (>10%; Table 7, Fig. 6) and membrane scaling were observed (Figs. 7 & 8) for the tests performed without AS feed treatment when $\overline{SI}_{M,G} \geq 1.9$ at the natural source water pH (for which $\overline{SI}_{M,C} \geq 4.2$) or when $\overline{SI}_{M,G} \geq 1.5$ at the reduced pH (for which $\overline{SI}_{M,C} \leq 0.37$). The greater extent of scaling and flux decline at the lower $\overline{SI}_{M,G}$ (< 2), observed at the reduced pH, is consistent with recent work on a similar water source [7]. It was shown in previous work that

the above behavior is associated with the reduction of the bicarbonate concentration (by at least an order of magnitude for the pH range of ~7.5–6.5 in the present study), thereby reducing the ability of bicarbonate to inhibit gypsum scaling.

For the RO tests performed for the three field source water samples having $SI_G \approx 1.0$ (VGD, LNW, and OAS) the percent flux decline and surface scale coverage (Table 7; Figs. 7 & 8) increased with increasing level of solution saturation at the membrane surface (or equivalent recovery; Table 7). Scale formation is more severe toward the downstream (or exit) region of the membrane channel (Fig. 8) which is consistent with the increased concentration along the membrane channel [21]. Comparison of the severity of mineral scaling in the RO channel exit region (Fig 8) was consistent with the degree of flux decline (Table 7). The results for the ERR water source were an exception having measurable flux decline (12% at t = 24 hr), but no visible surface scaling, but with a darkened membrane surface suggesting the possibility of organic fouling. The ERR water source had the highest TOC (total organic carbon) concentration (17 mg/L), relative to the other four sites (3–6 mg/L; Table 4), and thus the highest organic fouling potential of the studied sites.

The PFRO desalting tests demonstrated that, for SJV water sources evaluated in the present study, RO operation at the natural alkaline pH of the source water (where the solution is oversaturated with respect to calcite) would be preferable to operating at lower acidic pH (i.e., conditions of undersaturation with respect to calcite). Although one could operate at acidic pH, this would require higher antiscalant dosing (and thus higher desalination cost) to suppress gypsum scaling.

It should be recognized that even though the recovery level in the PFRO system is small (< 2%), the equivalent recovery in an actual RO plant can be estimated by assuming that the same level of concentration polarization level in the PFRO cell can be sustained in a full-scale

RO plant (for the tail-end elements). Accordingly, Eq. (1) can be used to estimate the equivalent recovery whereby *CF* is replaced by CP/α with $\alpha = 1.2$; when α is set to unity the assumption is that the plant operates such that the salt concentration is uniform across the membrane channel (a condition that would exist when the plant operates up to the thermodynamic limit [32]. The estimated equivalent recoveries (assuming $\alpha = 1$) were 38% and 45% for sites VGD and LNW, respectively, and 53% for sites ERR, CNR and OAS. Scale-free operation would be feasible without antiscalant use when operating at the natural source water pH for the CNR VGD and ERR sites at the above equivalent recoveries. Given that the LNW water source had a salinity (11,270 mg/L TDS) almost equal to that of the OAS water (11,020 mg/L TDS), a series of RO tests were performed with the LNW water at a slightly lower equivalent recovery (45%) for which a significant decrease in scaling was observed at both at the natural source water pH and at pH ~6.5. In addition, from a practical viewpoint, it is apparent that for the VGD water source (salinity of 28,780 mg/L TDS) achieving recovery approaching 70% would require applied pressure approaching or exceeding the rated pressure for the brackish RO elements (~ 4140 kPa or 600 psi).

The PFRO tests indicated that a low level of antiscalant dosing should make it possible to achieve scale-free desalting operation at the indicated recovery levels (Table 7), for the five water sources, at either the natural source water pH or under acidic pH. One is cautioned, however, that within the context of the present rapid PFRO diagnostic approach, acceptable operating conditions for full-scale plant operation should be established based on a criterion of no-flux decline (after accounting for the effect of membrane compaction) and verification of the absence of mineral scaling on the membrane surface. It is noted that the expected recovery levels for the five tested water sources are relatively low for inland water desalting. In order to minimize the brine management challenge and decrease overall water desalination cost, a higher

recovery level operation would be required. Indeed, recent studies indicate that higher recovery operation is feasible [10, 13, 33, 34]. In such a process, it is suggested that high recovery can be achieved by chemical demineralization of the primary RO (PRO) in an interstage crystallizer to reduce the concentration of mineral scale precursors, followed by filtration and subsequent desalting of the treated PRO in a secondary RO stage to increase the overall recovery.

5. Conclusions

The recovery limits of RO desalting of brackish agricultural drainage water in the San Joaquin Valley were evaluated based on field water quality monitoring data from various locations in the SJV, in addition to laboratory RO tests using field water samples. Analysis of DWR monitoring data revealed salinity in the different locations being in the range of 7000–23,000 mg/L TDS, with significant salinity variations of 12–52% relative to the 12-month averages. SJV brackish water was found to have a high mineral scaling propensity with the saturation indices for gypsum and calcite reaching levels as high as 0.99 and 5.3 respectively, with corresponding 12-month variations in the ranges of 5%–45% and 54%–92% (relative to the 12-month average for the different locations studied). Analysis of the RO recovery limits, based on historical water quality data (for five representative geographical locations) and experimental RO scaling tests with field data suggested expected RO product water recovery range of 44–68% across the SJV. Laboratory RO desalting tests in a diagnostic RO cell indicated that, in contrast to thermodynamic solubility analysis, which suggested lowering the feed pH to reduce calcite supersaturation, operation at the natural source water pH (~7.5–8) was preferable since it resulted in lower degree of membrane mineral scaling. Implementation of RO technology for desalination of SJV AD water would require site-specific RO process optimization given the geographical variability in water quality. Field evaluation of RO desalting with advanced mobile RO pilot plants [35] can provide the means for rapid optimization of RO operating conditions. Future

developments of RO technology for operation, under conditions of significant temporal variability of brackish water quality and desalting near the mineral scaling threshold (i.e., near the maximum allowable recovery in order to minimize brine generation), would require effective real-time methods of mineral scale detection [14, 36] and a plant operation that can be adjusted to mitigate mineral scaling (e.g., adjusting recovery and/or antiscalant dose or initiating membrane cleaning).

6. Acknowledgements

This work was supported, in part, by the California Department of Water Resources, the Metropolitan Water District of Southern California, the University of California Water Resources Center, the International Desalination Association, the U.S. Environmental Protection Agency, and the California Desalination Coalition.

References

[1] California Agricultural Resource Directory 2006, USDA, National Agricultural Statistics Service, California Department of Food and Agriculture, 2006.

[2] Assessing the Region Via Indicators: The Economy, Great Valley Center, Modesto, 2005.

[3] Evaluation of the 1990 Drainage Management Plan for the Westside San Joaquin Valley, California, San Jaoquin Valley Drainage Implementation Program and University of California Ad Hoc Coordination Committee, 2000.

[4] San Joaquin Valley Drainage Monitoring Program 2000, State of California, Department of Water Resources, September 2003 2003.

[5] Desalination Demonstration Report for Buena Vista Water Storage District, (2003).

[6] M.A. Clinton Williams, Agricultural Drainage in the San Joaquin Valley: A Gap Analysis, San Joaquin Valley Drainage Implementation Program, 2002.

[7] A. Rahardianto, B.C. McCool, and Y. Cohen, Reverse osmosis desalting of inland brackish water of high gypsum scaling propensity: Kinetics and mitigation of membrane mineral scaling, Environmental Science & Technology, 42 (2008) 4292.

[8] S. Gao, K.K. Tanji, R.A. Dahlgren, J. Ryu, M.J. Herbel, and R.M. Higashi, Chemical status of selenium in evaporation basins for disposal of agricultural drainage, Chemosphere, 69 (2007) 585.

[9] S.F.E. Boerlage, M.D. Kennedy, I. Bremere, G.J. Witkamp, J.P. Van der Hoek, and J.C. Schippers, The scaling potential of barium sulphate in reverse osmosis systems, Journal of Membrane Science, 197 (2002) 251.

[10] C.J. Gabelich, M.D. Williams, A. Rahardianto, J.C. Franklin, and Y. Cohen, High-recovery reverse osmosis desalination using intermediate chemical demineralization, Journal of Membrane Science, 301 (2007) 131.

[11] D. Hasson, A. Drak, and R. Semiat, Inception of CaSO4 scaling on RO membranes at various water recovery levels, Desalination, 139 (2001) 73.

[12] B.C. McCool, A. Rahardianto, and Y. Cohen, Technical and Economic Feasibility of Reverse Osmosis Reclamation of Agricultural Drainage Water in the San Joaquin Valley, Proceedings of the AIChE Annual Conference, 2006, San Francisco, CA.

[13] A. Rahardianto, J. Gao, C.J. Gabelich, M.D. Williams, and Y. Cohen, High recovery membrane desalting of low-salinity brackish water: Integration of accelerated precipitation softening with membrane RO, Journal of Membrane Science, 289 (2007) 123.

[14] M. Uchymiak, A. Rahardianto, E. Lyster, J. Glater, and Y. Cohen, A novel RO ex situ scale observation detector (EXSOD) for mineral scale characterization and early detection, Journal of Membrane Science, 291 (2007) 86.

[15] M. Brusilovsky, J. Borden, and D. Hasson, Flux decline due to gypsum precipitation on RO membranes, Desalination, 86 (1992) 187.

[16] S. Lee and C.-H. Lee, Effect of operating conditions on CaSO4 scale formation mechanism in nanofiltration for water softening, Water Research, 34 (2000) 3854.

[17] R.-W. Lee, J. Glater, Y. Cohen, C. Martin, K. Kovac, M.N. Milobar, and D.W. Bartel, Low-pressure RO membrane desalination of agricultural drainage water, Desalination, 155 (2003) 109.

[18] W.-Y. Shih, K. Albrecht, J. Glater, and Y. Cohen, A dual-probe approach for evaluation of gypsum crystallization in response to antiscalant treatment, Desalination, 169 (2004) 213.
[19] W.-Y. Shih, A. Rahardianto, R.-W. Lee, and Y. Cohen, Morphometric characterization of calcium sulfate dihydrate (gypsum) scale on reverse osmosis membranes, Journal of Membrane Science, 252 (2005) 253.
[20] R.Y. Ning, Discussion of silica speciation, fouling, control and maximum reduction, Desalination, 151 (2002) 67.
[21] E. Lyster and Y. Cohen, Numerical study of concentration polarization in a rectangular reverse osmosis membrane channel: Permeate flux variation and hydrodynamic end effects, Journal of Membrane Science, 303 (2007) 140.
[22] Hydranautics, Terms and Equations of Reverse Osmosis, (2001).
[23] I. Koch Membrane Systems, ROPRO 8.04. 2008.
[24] Hydranautics, Chemical Pretreatment of RO/NF, Technical Application Bulletin No. 111 Rev. C, 2008.
[25] OLI, OLI Analyzer 2.0. OLI Systems, Morris Plains, NJ, 2005.
[26] Kurt Kovac, Jose Faria, Tony Lam, and D. Lara, Drainage water samples and laboratory reports, Brian C McCool and Y. Cohen, Editors. 2006-2007: Los Angeles, CA.
[27] AWWA, Standard Methods for the Examination of Water and Wastewater, 20th ed., American Public Health Association, Washington, DC, 1998.
[28] USEPA. Clean Water Act Analytical Methods: Approved General-Purpose Methods. 2010 [cited 2010; Available from: http://www.epa.gov/waterscience/methods/method/.
[29] D. Norberg, S. Hong, J. Taylor, and Y. Zhao, Surface characterization and performance evaluation of commercial fouling resistant low-pressure RO membranes, Desalination, 202 (2007) 45.
[30] A. Rahardianto, W.-Y. Shih, R.-W. Lee, and Y. Cohen, Diagnostic characterization of gypsum scale formation and control in RO membrane desalination of brackish water, Journal of Membrane Science, 279 (2006) 655.
[31] Selection of Candidate Sumps to Determine Critical Membrane Desalination Process Requirements. 2004, California Department of Water Resources.
[32] A. Zhu, P.D. Christofides, and Y. Cohen, On RO membrane and energy costs and associated incentives for future enhancements of membrane permeability, Journal of Membrane Science, 344 (2009) 1.
[33] A. Rahardianto, B.C. McCool, and Y. Cohen, Accelerated Desupersaturation of Reverse Osmosis Concentrate by Chemically-Enhanced Seeded Precipitation (in Press), Desalination (2010).
[34] A. Zhu, A. Rahardianto, P.D. Christofides, and Y. Cohen, Reverse Osmosis Desalination with High Permeability Membranes - Cost Optimization and Research Needs (*in Press*), Desalination and Water Treatment (2010).
[35] M. Uchymiak, A.R. Bartman, N. Daltrophe, M. Weissman, J. Gilron, P.D. Christofides, W.J. Kaiser, and Y. Cohen, Brackish water reverse osmosis (BWRO) operation in feed flow reversal mode using an ex situ scale observation detector (EXSOD), Journal of Membrane Science, 341 (2009) 60.
[36] A.R. Bartman, C.W. McFall, P.D. Christofides, and Y. Cohen, Model-predictive control of feed flow reversal in a reverse osmosis desalination process, Journal of Process Control, 19 (2009) 433.

LIST OF TABLES

Table 1. Summary of average water quality and saturation indices for the most recent 12-month period of available data from the DWR database (2003–2004)

Table 2. Variability of water quality measurements and saturation indices for the OAS location

Table 3. Summary of water quality and saturation indices for the collected field water samples (2006–2007) †

Table 4. Detailed water quality analyses for five location in the SJV sampled during 2006–2007

Table 5. Recovery limits for water samples having the maximum and minimum TDS observed during the most recent 12-month period of reported data.

Table 6. Recovery limits estimated based on water quality analysis of field water samples

Table 7. Diagnostic flux decline experimental conditions and 24-hour flux decline

LIST OF FIGURES

Figure 1. San Joaquin Valley (SJV) field water sampling locations: OAS (1), VGD (2), ERR (3), LNW (4), & CNR (5).

Figure 2. Saturation indices as a function of recovery for OAS water field water (11020 mg/L TDS, sampled on 4/10/2006, calculated based on 98% salt rejection)

Figure 3. Saturation indices as a function of pH for OAS field water (11020 mg/L TDS, sampled on 4/10/2006)

Figure 4. Gypsum saturation index at the membrane surface as a function of recovery for OAS field water (sampled on 4/10/2006) illustrating the effect of concentration polarization (i.e., increasing with α value; Eq. 5)

Figure 5. Illustration of water quality variations for the 2003–2004 period in the DWR database [4] and for the 2006 field samples: (a) at the OAS site, (b) at the CNR site, and (c) at the LNW site.

Figure 6. Permeate flux (ratio of the flux at time t, J_t, to the initial flux, J_0, respectively) for 24-hr scaling tests at the natural pH of the field water and at an acidic pH for: (a) OAS, (b) CNR, and (C) LNW; and at an acidic pH with AS addition (0.2 ppm PC-504) for (a) OAS, and (b) CNR.

Figure 7. Examples of membrane coupons images after 24-hour scaling tests on field water samples from: (a) OAS at the natural pH=7.42, (b) OAS at an acidic pH=5.47, (c) LNW at the natural pH=7.43, and (d) LNW at an acidic pH=6.48.

Figure 8. Images of the membrane coupon exit regions after 24-hr scaling tests (see Table 7).

Table 1. Summary of average water quality and saturation indices for the most recent 12-month period of available data from the DWR database (2003–2004)

Name	Location	TDS, mg/L	pH	π_0†, kPa	SI_C†	SI_G†
OAS	Central Area	7,999	7.7	408	3.9	**0.75**
LNW	Southern Area, Lost Hills	11,944	7.5	834	2.3	**0.99**
CNR	Southern Area, Kern Lake Bed	6,987	7.7	315	5.1	0.76
VGD	Southern Area, Lemoore	**23,480**	7.9	1000	5.3	0.84

† π_0, SI_C, and SI_G were calculated at 20 °C.

Table 2. Variability of water quality measurements and saturation indices for the OAS location

Date	7/14/2003	9/9/2003	11/12/2003	1/12/2004	3/22/2004	5/10/2004	Average
TDS, mg/L	5,864	**3,828**	9,344	**11,100**	9,576	8,284	7,999
$[Ca^{2+}]$, mg/L	283	224	385	430	454	358	356
$[SO_4^{2-}]$, mg/L	3,990	2,340	5,550	6,460	5,630	4,890	4,810
Total Alkalinity, mg/L as $CaCO_3$	271	239	160	173	146	217	201
pH	7.6	**7.1**	**7.9**	**7.9**	**7.9**	**7.9**	7.7
π_0†, kPa	371	231	466	534	443	407	409
SI_C†	3.2	**0.86**	4.3	4.7	4.5	**5.8**	3.9
SI_G†	0.57	**0.41**	0.83	0.93	**0.98**	0.76	0.75

† π_0, SI_C, and SI_G were calculated at 20 °C.

Table 3. Summary of water quality and saturation indices for the collected field water samples (2006–2007) †

Name	Location	Sample Date	TDS, mg/L	pH	π_0†, kPa	SI_C†	SI_G†	SI_S†
OAS	Central Area	4/10/2006	11020	7.6	515	3.0	0.99	0.29
LNW	Southern Area, Lost Hills	2/15/2006	11270	7.6	723	2.7	1.03	0.35
CNR	Southern Area, Kern Lakebed	7/31/2006	6372	7.5	286	2.7	0.70	0.22
VGD	Southern Area, Lemoore	11/13/2006	28780	7.6	1320	2.2	0.95	0.38
ERR	Southern Area, Corcoran	1/29/2007	4115	8.0	265	9.5	0.12	0.34

† π_0, SI_C, and SI_G were calculated at 20 °C.

Table 4. Detailed water quality analyses for five location in the SJV sampled during 2006–2007

Measurement	Units	Location				
		CNR	**LNW**	**OAS**	**VGD**	**ERR**
Conductance	µS/cm	7111	14430	12620	26070	5580
pH	pH units	7.5	7.6	7.6	7.6	8
UV Absorbance (254 nm)	absorbance/cm	0.13	0.09	0.13	0.18	0.59
Dissolved Measurements						
Bicarbonate	mg/L as $CaCO_3$	229	128	212	367	699
Boron	mg/L	13.5	17.5	23.5	43.4	2.6
Calcium	mg/L	350	625	462	422	88
Carbonate	mg/L as $CaCO_3$	1*	1*	1*	1*	7
Chloride	mg/L	324	3020	1060	1910	632
Fluoride	mg/L	5*	10*	10*	5*	5*
Hydroxide	mg/L as $CaCO_3$	1*	1*	1*	1*	1*
Magnesium	mg/L	236	198	284	962	59
Nitrate	mg/L	344	155	47	52	51
DOC	mg/L as C	4.2	4.6	5.1	6.2	15.8
Potassium	mg/L	46.7	5*	5*	7.8	3.5
Selenium	mg/L	0.03	0.22	0.18	0.05*	0.01
Silica	mg/L	24	38	31	43	38
Sodium	mg/L	1250	2820	2780	9270	1250
Sulfate	mg/L	3700	4520	6360	21400	1570
Total Measurements						
Total Alkalinity	mg/L as $CaCO_3$	230	128	213	368	706
Aluminum	mg/L	0.1*	0.1*	0.05*	0.5*	0.102
Arsenic	mg/L	0.01*	0.014	0.006	0.05*	0.089
Barium	mg/L	0.5*	0.5*	0.25*	2.5*	0.5*
TDS	mg/L	6372	11270	11020	28780	4115
Iron	mg/L	0.17	0.15	0.05	1.4	0.28
Manganese	mg/L	0.05*	0.05*	0.025*	1.55	0.60
TOC	mg/L as C	4.5	3.4	5.1	6.2	16.7
Phosphorus	mg/L	0.01*	0.03	0.08	0.12	1.96
Selenium	mg/L	0.034	0.235	0.195	0.05*	0.013
Strontium	mg/L	17.2	10.0	5.5	9.6	0.9
TSS	mg/L	1*	4	4	2	4

* Measured value is at or below reporting limit.

Table 5. Recovery limits for water samples having the maximum and minimum TDS observed during the most recent 12-month period of reported data.

Site	Sample Date	TDS, mg/L	Recovery Limits				
			Pressure	calcite (pH 7.5)	calcite (pH 6.0)	gypsum (pH 6.0)	gypsum (pH 6.0)
			π = 60800 kPa	SI = 1	SI = 1	SI = 1	SI = 2.3
OAS	1/12/2004	11100	86–88%	0* %	92–93%	0* %	47–56%
OAS	9/9/2003	3828	94–95%	0* %	88–90%	44–53%	76–80%
LNW	9/9/2003	13400	76–80%	0* %	84–86%	0* %	43–53%
LNW	7/28/2003	11030	75–80%	0* %	85–87%	0*–0.002%	46–55%
CNR	11/12/2003	9136	90–91%	0* %	83–86%	8.6–24%	62–68%
CNR	7/28/2003	4660	93–94%	0* %	86–88%	3.7–19%	57–64%
VGD	1/13/2004	29760	68–73%	0* %	89–91%	0*–7.6%	61–68%
VGD	7/29/2003	14110	77–80%	0* %	90–92%	3.6–18%	65–71%

Note: Bold values are the recovery limits with pH adjustment and antiscalant use. The given ranges indicate the minimum and maximum expected recoveries (i.e. for α=1.2 or 1.0, respectively; see Eq. 5). (*) indicates that the feed is oversaturated at the membrane surface.

Table 6. Recovery limits estimated based on water quality analysis of field water samples

Site	TDS, mg/L	Nat pH	Recovery Limits					
			Pressure (nat. pH)	calcite (nat. pH)	calcite (pH 6)	gypsum (pH 6)	gypsum (pH 6)	silica (pH 6)
			π = 60800 kPa	SI_c = 1	SI_c = 1	SI_g = 1	SI_g = 2.3	SI_s = 1
OAS	11,020	7.6	87–89%	0^* %	89–91%	0^*–0.7%	49–**58%**	63–69%
LNW	11,270	7.6	80–83%	0^* %	88–90%	oversat.	44–**54%**	54–62%
CNR	6,372	7.5	93–94%	0^* %	89–91%	13–27%	62–**68%**	72–77%
VGD	28,780	7.6	64–70%	0^* %	89–91%	0^*–6.2%	60–67%	46–**55%**
ERR	4,116	8.0	93–94%	0^* %	86–88%	82–85%	93–94%	56–**63%**

Note: Bold values are the recovery limits with pH adjustment and antiscalant use. The given ranges indicate the minimum and maximum expected recoveries (i.e. for α=1.2 or 1.0, respectively; see Eq. 5). (*) indicates that the feed is oversaturated at the membrane surface.

Table 7. Diagnostic flux decline experimental conditions and 24-hour flux decline

Site	**Condition**	**pH**	***P*, kPa**	***u*, cm/s**	$J_0 \cdot 10^3$**, cm/s**	$SI_{M,C}$	$SI_{M,G}$	$SI_{M,S}$	FD_{24}	ϕ_{24}	Y_{eqv} α =1.2–1
OAS	Nat. pH	7.42	2500	19.1	2.45	5.4	2.1	0.61	11 %	12%	43–53%
OAS	Low pH	5.47	2580	19.1	2.45	0.014	2.1	0.66	47 %	65%	43–53%
OAS	Low pH & AS	5.94	2410	19.1	2.44	0.86	2.1	0.66	7.9 %	0%	44–53%
CNR	Nat. pH	7.50	1920	19.1	2.44	7.4	1.53	0.46	6.4 %	2.5%	44–53%
CNR	Low pH	5.27	1860	19.1	2.44	0.01	1.55	0.49	11 %	3.8%	44–53%
CNR	Low pH & AS	6.00	2010	19.1	2.44	0.11	1.55	0.49	6.7 %	0%	44–53%
ERR	Nat. pH	8.02	2080	19.1	2.446	29	0.28	0.68	12 %	0%	44–53%
ERR	Low pH	5.37	2110	19.1	2.44	0.01	0.31	0.79	12 %	0%	44–53%
ERR	Low pH & AS	6.00	1900	19.1	2.44	0.13	0.30	0.79	7.5 %	0%	44–53%
LNW	Nat. pH	7.43	1930	25.1	1.91	4.2	1.9	0.64	11 %	5.7%	34–45%
LNW	Low pH	6.48	1950	25.1	1.89	0.37	1.9	0.68	14 %	7.6%	34–45%
VGD	Nat. pH	7.53	3120	19.1	1.36	3.2	1.4	0.61	8.0 %	1.8%	26–38%
VGD	Low pH	5.56	2980	19.1	1.35	0.01	1.4	0.71	8.9 %	0.5%	25–38%
VGD	Low pH+AS	5.93	3140	19.1	1.36	0.05	1.4	0.72	9.4 %	0%	26–38%

Note: $SI_{M,C}$, $SI_{M,G}$, and $SI_{M,S}$ are the initial average saturation indices for calcite, gypsum and silica at the membrane surface; u is the cross-flow velocity of the feed; P is the applied pressure; Y_{eqv} is the equivalent recovery in for an RO plant (Eq 1) with the given ranges indicating the minimum and maximum expected recoveries (i.e. for α=1.2 or 1.0, respectively; see Eq. 1).

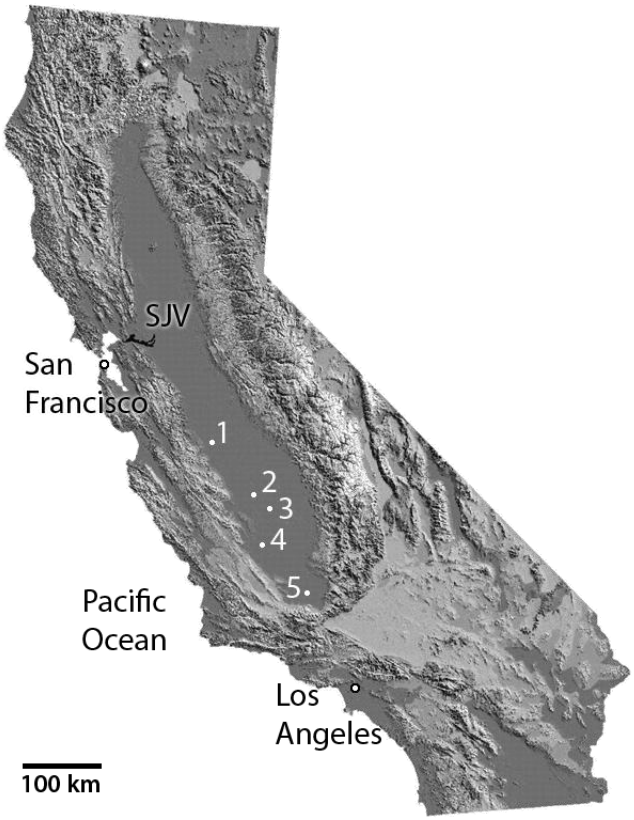

Figure 1. San Joaquin Valley (SJV) field water sampling locations: OAS (1), VGD (2), ERR (3), LNW (4), & CNR (5).

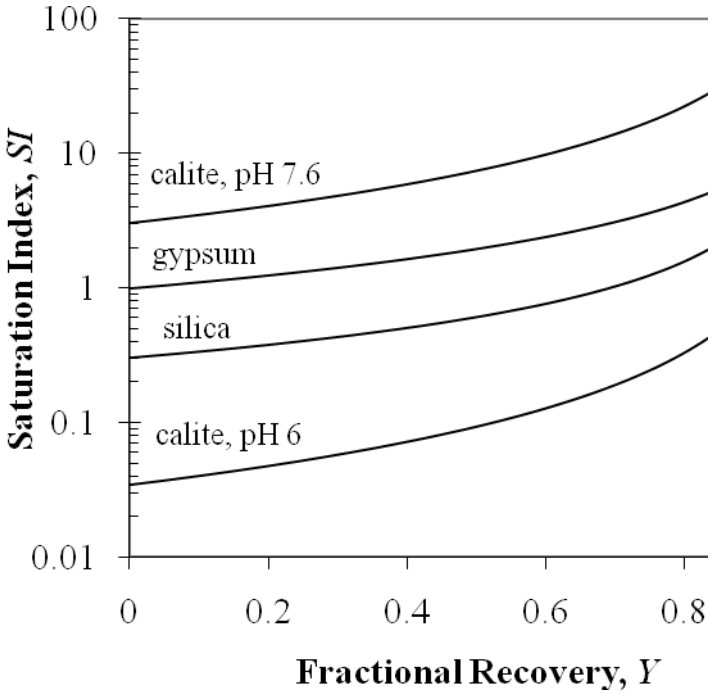

Figure 2. Saturation indices as a function of recovery for OAS water field water (11020 mg/L TDS, sampled on 4/10/2006, calculated based on 98% salt rejection)

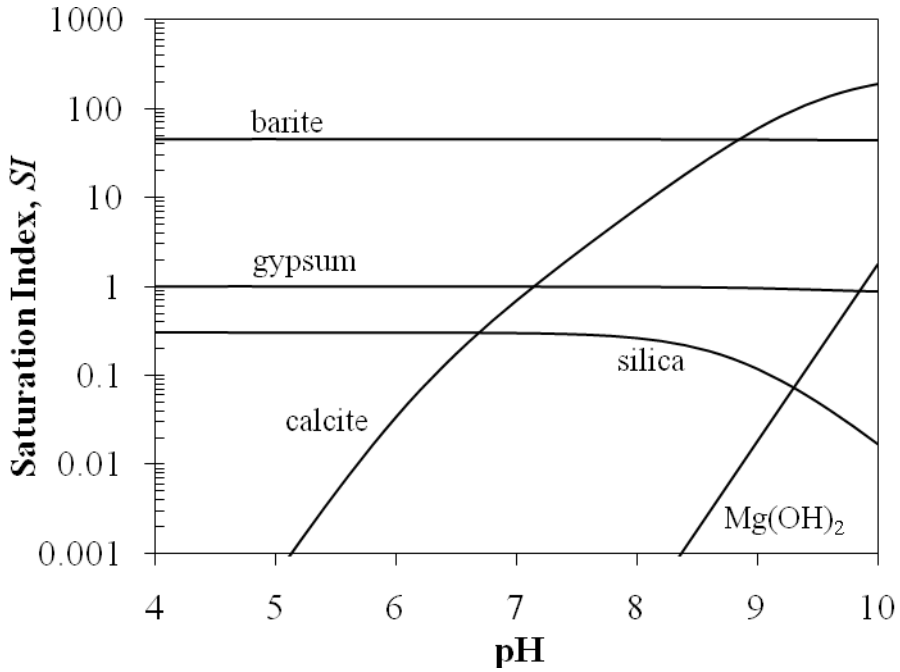

Figure 3. Saturation indices as a function of pH for OAS field water (11020 mg/L TDS, sampled on 4/10/2006)

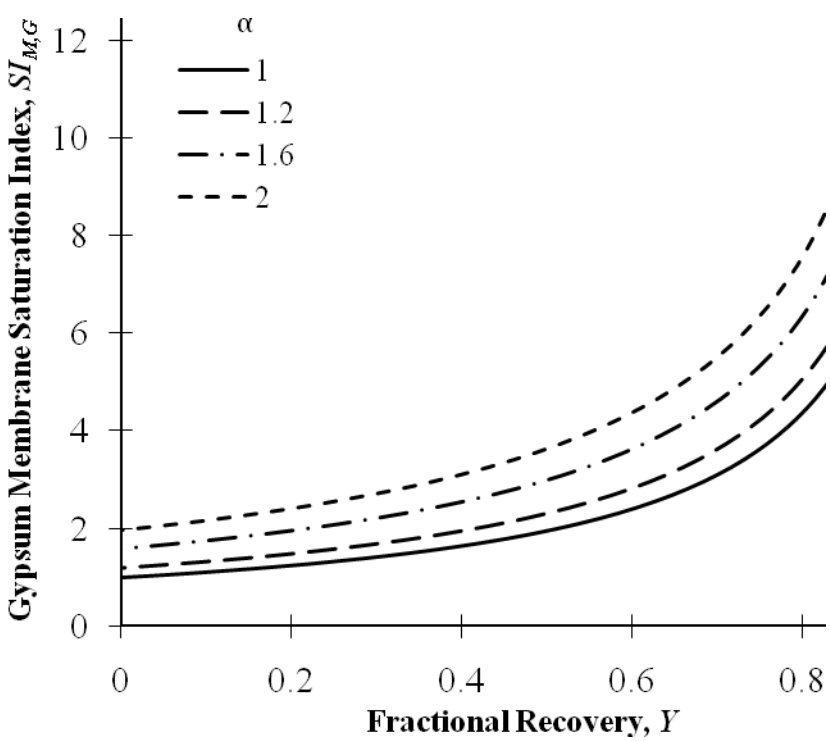

Figure 4. Gypsum saturation index at the membrane surface as a function of recovery for OAS field water (sampled on 4/10/2006) illustrating the effect of concentration polarization (i.e., increasing with α value; Eq. 5)

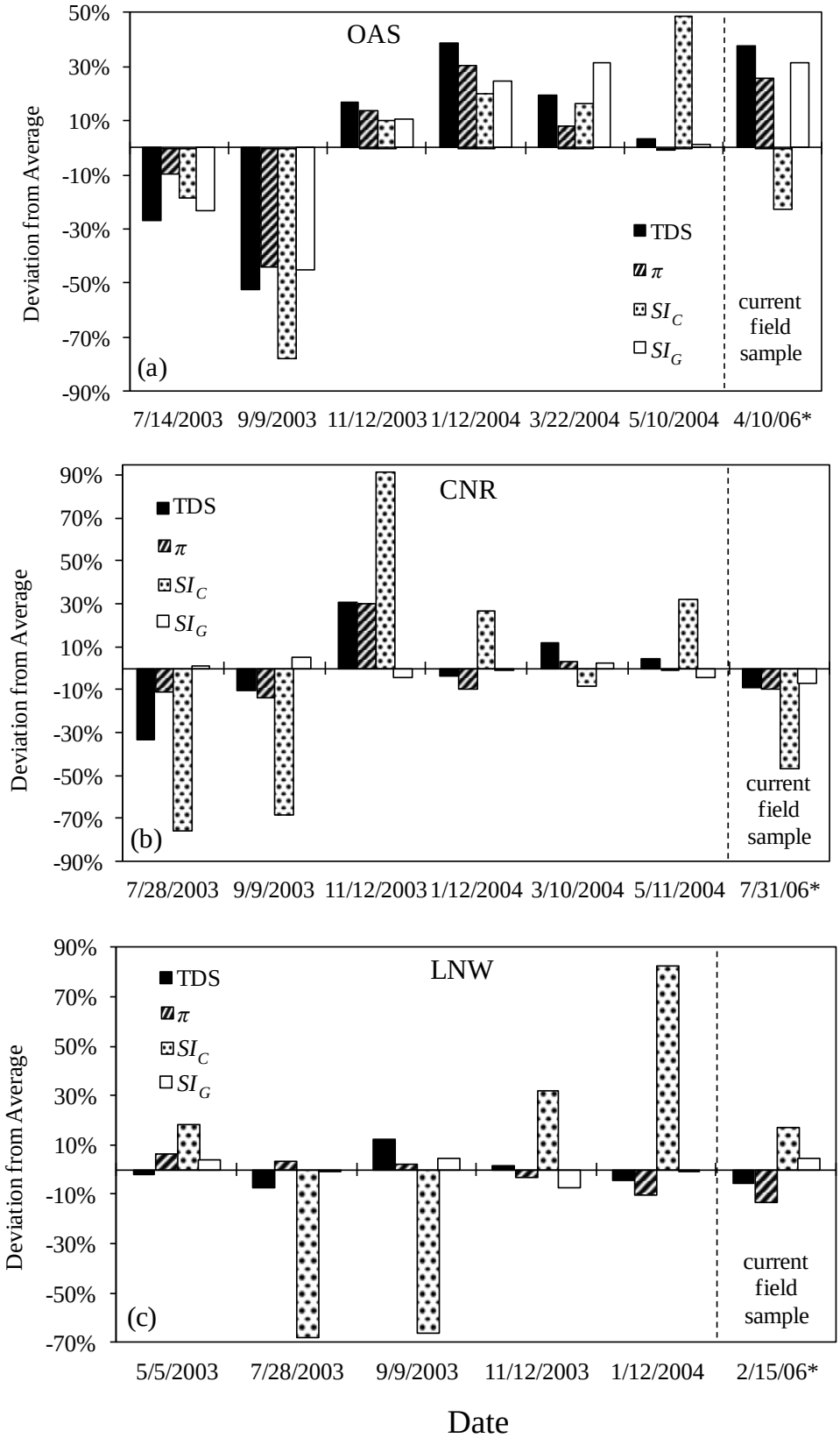

Figure 5. Illustration of water quality variations for the 2003–2004 period in the DWR database [4] and for the 2006 field samples: (a) at the OAS site, (b) at the CNR site, and (c) at the LNW site.

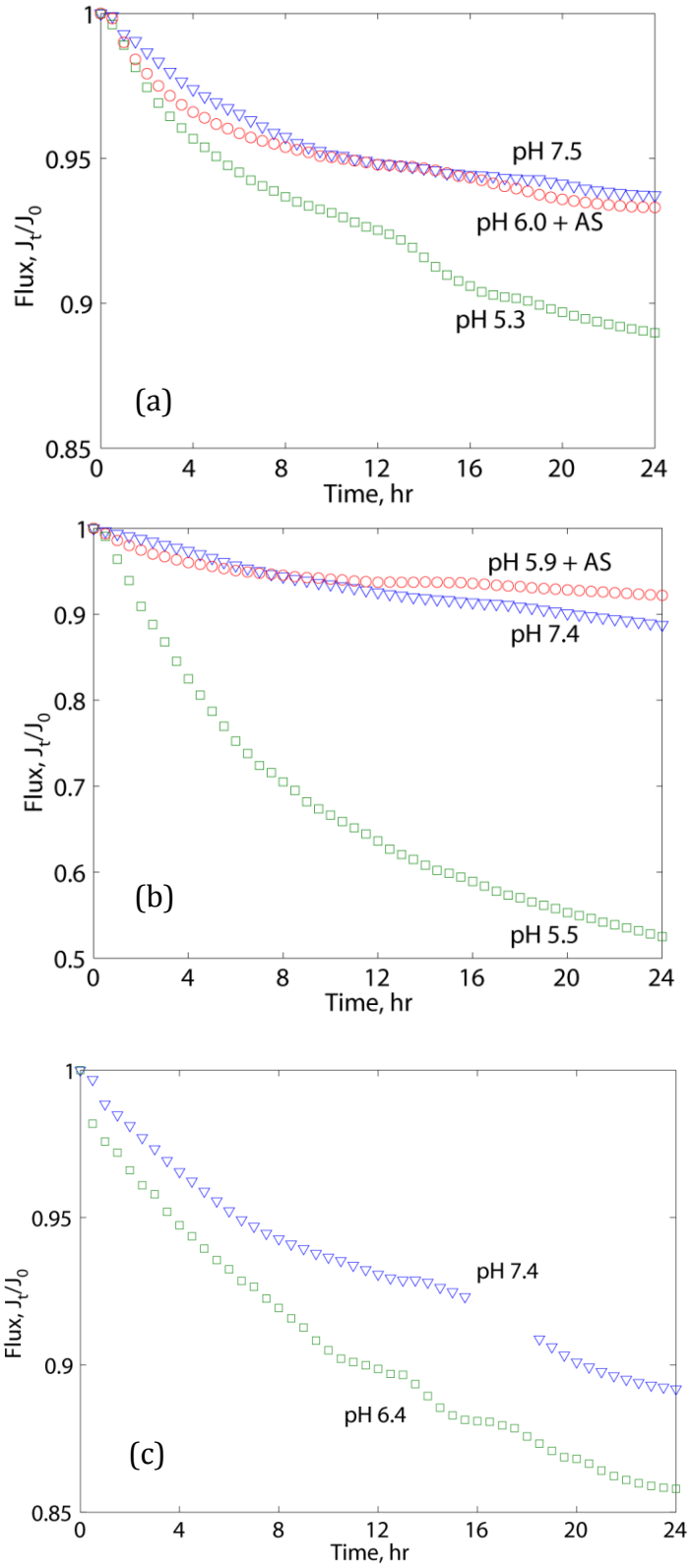

Figure 6. Permeate flux (ratio of the flux at time t, J_t, to the initial flux, J_0, respectively) for 24-hr scaling tests at the natural pH of the field water and at an acidic pH for: (a) OAS, (b) CNR, and (C) LNW; and at an acidic pH with AS addition (0.2 ppm PC-504) for (a) OAS, and (b) CNR.

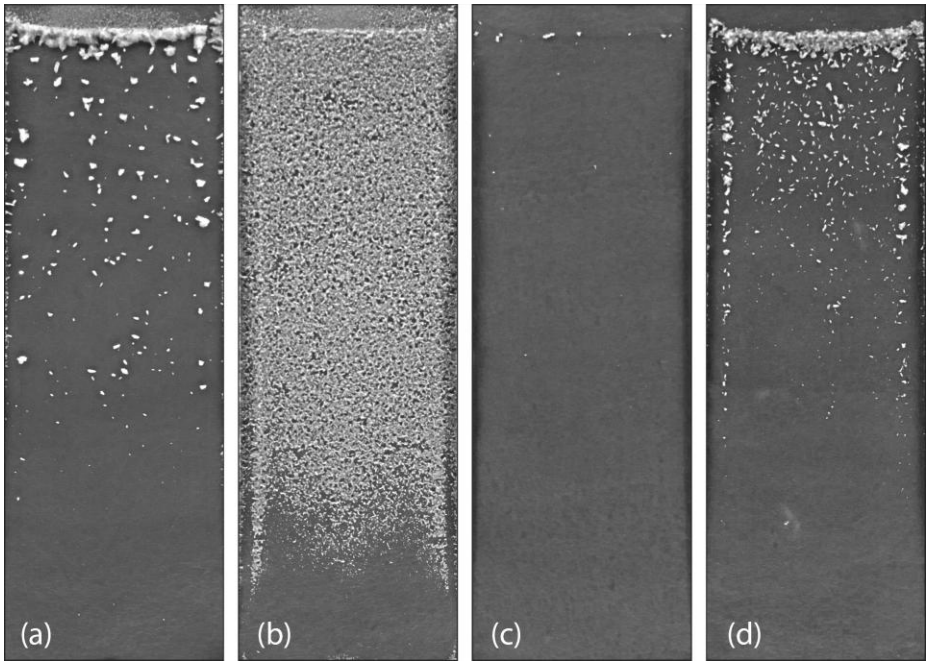

Figure 7. Examples of membrane coupons images after 24-hour scaling tests on field water samples from: (a) OAS at the natural pH=7.42, (b) OAS at an acidic pH=5.47, (c) LNW at the natural pH=7.43, and (d) LNW at an acidic pH=6.48.

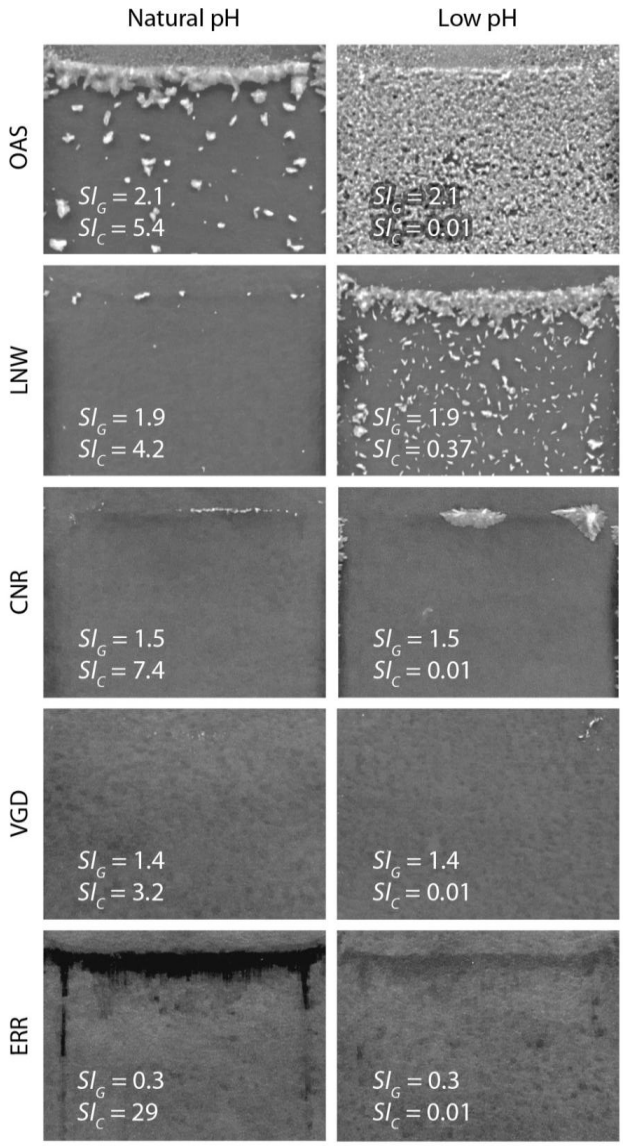

Figure 8. Images of the membrane coupon exit regions after 24-hr scaling tests (see Table 7).